Comparison of the Human and Worm p53 Structures Suggests a Way for Enhancing Stability†

Yongping Pan,‡ Buyong Ma,‡ Arnold J. Levine,§ and Ruth Nussinov*,‡,||

Basic Research Program, SAIC−Frederick, Inc., Center for Cancer Research Nanobiology Program, NCI−Frederick, Frederick, Maryland 21702, Institute for Advanced Study, Einstein Drive, Princeton, New Jersey 08540, and Sackler Institute of Molecular Medicine, Department of Human Genetics and Molecular Medicine, Sackler School of Medicine, Tel Aviv University, Tel Aviv 69978, Israel

Received November 2, 2005; Revised Manuscript Received January 23, 2006

ABSTRACT: Maintaining the native conformation is essential for the proper function of tumor suppressor protein p53. However, p53 is a low-stability protein that can easily lose its function upon structural perturbations such as those resulting from missense mutations, leading to the development of cancer. Therefore, it is important to develop strategies to design stable p53 which still maintains its normal function. Here, we compare the stabilities of the human and worm p53 core domains using molecular dynamics simulations. We find that the worm p53 is significantly more stable than the human form. Detailed analysis of the structural fluctuations shows that the stability difference lies in the peripheral structural motifs that contrast in their structural features and flexibility. The most dramatic difference in stability originates from loop L1, from the turn between helix H1 and β-strand S5, and from the turn that connects β-strands S7 and S8. Structural analysis shows significant differences for these motifs between the two proteins. Loop L1 lacks secondary structure, and the turns between helix H1 and strand S5 and between strands S7 and S8 are much longer in the human form p53. On the basis of these differences, we designed a mutant by shortening the turn between strands S7 and S8 to enhance the stability. Surprisingly, this mutant was very stable when probed by molecular dynamics simulations. In addition, the stabilization was not localized in the turn region. Loop L1 was also significantly stabilized. Our results show that stabilizing peripheral structural motifs can greatly enhance the stability of the p53 core domain and therefore is likely to be a viable alternative in the development of stable p53. In addition, loop- or turn-related mutants with different stabilities may also be used to probe the relationship between function, a particular structural motif, and its flexibility.

Tumor-suppressor protein p53 is involved in many important cellular functions (*1*). It responds to DNA damage and other cellular stress by triggering cell cycle arrest or apoptosis and thus is generally considered to be the guardian of the genome (*2*−*4*). The maintenance of these important cellular functions requires the structural integrity and proper population of the native state. Unfortunately, nonfunctional mutant p53 has been identified in more than half of all human cancers (*5*−*7*), mostly due to mutations leading to altered stability. The fact that so often a nonfunctional mutant is involved in cancer is related to the intrinsic low stability of the p53 protein (*8*), making its native conformation venerable to mutations at various positions. Evidence shows that while some of the mutations cause direct alteration at the DNA binding site, many others cause perturbation of the native conformation either globally (*9*−*12*) with an increased population of alternate conformations that differ in their DNA binding interfaces (*13*, *14*) or in various other regions (*15*). Therefore, novel approaches that can stabilize p53 and rescue its function are desired.

p53 has three domains: the N-terminal domain, the DNA binding core domain, and the C-terminal tetramerization domain (*13*, *16*). Most of the missense, cancer-related mutations have been mapped to the core domain (*6*). Studies of the relationships between specific mutations and their effect on protein function and between structure and function further indicate that the p53 core domain is much more sensitive to residue substitutions than the N- and C-terminal domains (*17*). Consequently, several approaches aiming at the stabilization of the p53 structure to rescue its functions have focused on this domain. These approaches include the design of small molecules or peptides that bind to it (*15*, *18*−*20*), introduction of another mutation (*21*, *22*), genetic in vitro evolution (*23*), or design of new mutants by

† This research was supported (in part) by the Intramural Research Program of the NIH, National Cancer Institute, Center for Cancer Research. This project has been funded in whole or in part with Federal funds from the National Cancer Institute, National Institutes of Health, under Contract NO1-CO-12400. The content of this publication does not necessarily reflect the views or policies of the Department of Health and Human Services, nor does mention of trade names, commercial products, or organizations imply endorsement by the U.S. Government. The research of R.N. in Israel has been supported in part by the Center of Excellence in Geometric Computing and its Applications, funded by the Israel Science Foundation. This study utilized the high-performance computational capabilities of the Biowulf PC/Linux cluster at the National Institutes of Health, Bethesda, MD (http://biowulf.nih.gov).

* Address correspondence to this author at NCI−Frederick. Tel: 301-846-5579. Fax: 301-846-5598. E-mail: ruthn@ncifcrf.gov.

‡ NCI−Frederick.

§ Institute for Advanced Study.

|| Tel Aviv University.

10.1021/bi052242n CCC: $33.50
Published on Web 03/04/2006

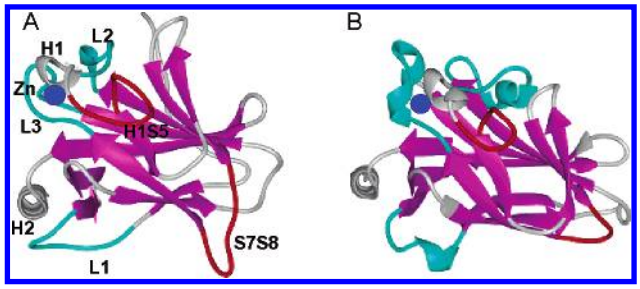

FIGURE 1: Ribbon representation of the crystal structures of the p53 core domain from human (A) and from worm (B) to highlight the structural similarity and differences. The two proteins have the same overall topology and folds organized against the β-sheet core scaffolds (pink), the three loops in the worm have higher contents of helical component (cyan), and two flexible turns, H1S5 and S7S8 (red), in the human p53 are longer than in the worm p53.

combining known stabilizing mutations (*24*, *25*). The latter approach was based on molecular evolution, which yielded a superstable quadruple mutant M133L/V203A/N239Y/N268D (*24*). This mutant is not only functional but also structurally very similar to the wild type as revealed by crystallography (*25*). This highlights the importance of the maintenance of the native conformation and the feasibility of a stable mutant design.

The major structural features of the p53 core domain have been characterized previously (*26*). The main frame of the core domain consists of two β-sheets packed against each other, with a Zn-centered region and helix H2 packed against it (Figure 1). These β-sheets serve as the scaffold for the core domain. Crystallography reveals that they are essential for the overall stability due to the main chain hydrogen bonding and the hydrophobic packing among the side chains (*25*). Although the stability and structural integrity of the p53 core domain can be easily damaged by perturbations in the β-sheets as observed in the study of the temperature-sensitive missense mutations (*27*), there is little room to enhance the stability by introducing better residue packing within the already highly packed β-sheets. On the other hand, the peripheral regions including loops and turns are loosely packed against each other or against the β-sheet core (Figure 1) and consequently often display higher mobility. Reducing the flexibility of these mobile regions could potentially enhance the overall stability of the protein. In addition, most missense mutations in these regions do not result in significant loss of p53 functions, relative to the conserved or more structured motifs, making them suitable for mutational engineering.

While the peripheral regions can be interesting targets for stabilization, it is not clear which particular regions can be engineered to enhance stability and how much the flexibility of a mobile region can be reduced while still retaining its biological functions, as it is known that some extent of the flexibility is required for protein function. Recently, a p53 homologue from *Caenorhabditis elegans* has been solved (*28*). The *C. elegans* p53 has functions similar to those of the human p53, including specific DNA binding and transcriptional activity upon various cell stresses (*29*−*31*). Comparison of the human and worm p53 structures reveals several differences in the peripheral regions. In the human p53, there are three large loops. While these loops still exist in the worm p53, part of each of the loops becomes a helix turn. Our molecular dynamics (MD)[1] simulations reveal that the worm p53 is much more stable than the human form. Because the two forms of p53 have essentially conserved topology and the same overall structure, such a correlation between the structures and stability motivated us to further explore the relationship between the differences in structure and stability. We show that the stability difference between the core domain of the human p53 and that of the worm p53 was the outcome of the difference in fluctuations of the peripheral motifs, while the β-sheet core retained its integrity early in the trajectories. Therefore, the loops and turns may have played important roles in the stability of p53, and their high flexibility might be responsible for the population of non-native conformations. We identify the most flexible regions and propose that these regions can be targets for stabilizing mutations. To illustrate the success of such a strategy, we design a mutant by shortening a turn that links β-strands S7 and S8. We show that reducing its size can significantly increase the stability of the protein core domain. Such engineered stable p53 mutants may have potential application in cancer therapy as well as for probing the roles of different flexible regions in maintaining the stability and the involvement in various protein−protein interactions.

METHODS

The structures used for simulations are the human p53 core domain (chain A in PDB file 1tsr, referred as p53h) and the worm p53 core domain (PDB file 1t4w, referred as p53w). The mutant with shortened S7S8 turn was built from the wild-type human form by removing the most flexible five residues (Glu224, Val225, Gly226, Ser227, and Asp228) in the turn (Figure 1A). To facilitate the resealing between residues Pro223 and Cys229, Pro223 was also mutated to Ala. The structure of the designed mutant was first minimized for 500 steps with the steepest decent algorithm with the backbone of the protein restrained before being subjected to the following system setup and production runs. Previously we have shown that MD simulations can be used as a measure for protein stability (*32*). The same protocol is used in this work. Briefly, MD simulations were performed using the CHARMM program (*33*) with the CHARMM 22 force field (*34*). Each system was solvated under neutral pH in a TIP3P (*35*) water box with a minimum distance of 10 Å from any edge of the box to any protein atom. The positive charges in the system were balanced by adding chloride ions. The solvated system was minimized for 500 steps with the protein restrained, followed by an additional 500 steps of minimization for the whole system to eliminate any residual unfavorable interactions between the solvent and the protein. The systems were then equilibrated for 20 ps with the NVT ensemble before the production simulations, which lasted for 5 ns with the NPT ensemble at temperatures of 300 and 325 K. During the simulations, the distances between the zinc ion and the coordinating atoms from three Cys residues and one His residue were restrained within ±0.2 Å of the crystal distance with the NOE module implemented in CHARMM. A time step of 2 fs and a nonbonded cutoff of 12 Å were used in the trajectory production.

[1] Abbreviations: MD, molecular dynamics; p53h, human p53; p53w, worm p53; RMSD, root-mean-square deviation.

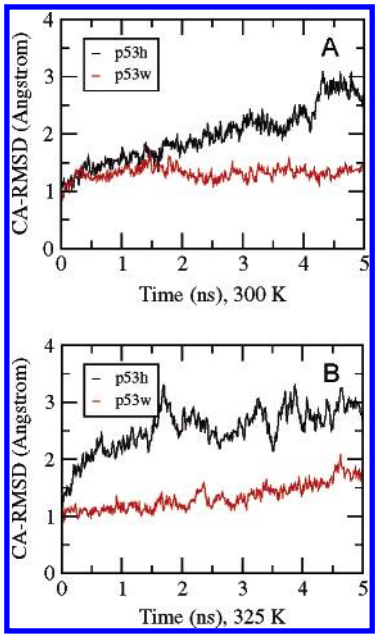

FIGURE 2: Cα atom root-mean-square deviations (RMSD) derived from simulations at 300 and 325 K from both the human p53 (p53h) and worm p53 (p53w) core domain from their crystal structures, respectively. The plots show that p53h is very unstable at both temperatures while p53w was stable even at elevated temperature. The three terminal residues at both the N- and C-termini were excluded in the calculations.

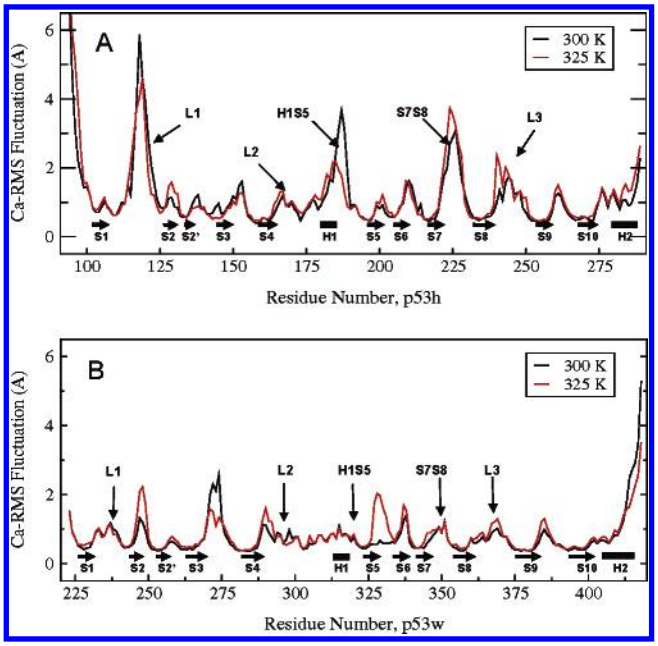

FIGURE 3: Residue-based Cα atom root-mean-square fluctuations for the human p53 (p53h) and the worm p53 (p53w) derived from the simulations in Figure 2. This figure allows the direct comparison of fluctuations for specific regions from the human and worm form proteins. Locations of the secondary structures are labeled with horizontal arrows for β-strands and rectangular bars for α-helices. Regions with the most dramatic contrast in fluctuation between p53h and p53w are indicated with thin arrows.

RESULTS

Stability Difference between the Human and Worm p53. Previously we have shown that MD simulations can be applied to qualitatively measure the difference in protein stability (*32*). Here again the MD protocol was used to characterize the stability properties of the two proteins. Because the total number of residues of the core domains of the human p53 (p53h) and *C. elegans* p53 (p53w) are very close to each other (194 residues for p53h and 196 residues for p53w), the structural fluctuations can be compared directly on the basis of information such as RMSD. Figure 2 shows the structural fluctuation difference between the two proteins. At 300 K, after the initial equilibration for about 300 ps, p53w displayed a high stability with the structure difference from the crystal structure remaining around 1.3 Å for the rest of the 5 ns trajectory (Figure 2A). In contrast, p53h displayed its instability with a continued increase in the structure fluctuations. At 325 K, p53w was able to remain very close to the crystal structure during 2 ns. Although the fluctuation increased gradually, the overall stability is still high compared with p53h, reaching only 1.75 Å at the end of the 5 ns trajectory. For p53h, the RMSD quickly reached 2 Å within the initial 0.5 ns at 325 K (Figure 2B). From the changes in the fluctuations upon an increase in temperature, it is clear that the structure of p53h is much more venerable to temperature increase than that of p53w. These results demonstrate the dramatic difference in stability between the two proteins. Because p53h and p53w have the same topology and similar structural motifs, detailed comparison of the fluctuations of corresponding structural motifs from the two proteins can yield insight into the factors that affect the overall stability of the protein, benefiting the design of stable human p53 mutants.

Peripheral Motifs Are the Major Elements for Stability Difference. The significant difference in the overall structural fluctuation between p53h and p53w was further dissected into residue-based fluctuations. Figure 3 shows the fluctuations for each individual residue. The relative magnitude of the fluctuations is in good agreement with the *B*-factors determined by X-ray crystallography. The figure shows that the β-strands that comprise the core frame of the proteins were consistently stable, with RMSD around 0.5 Å, while loops and turns were in general much more flexible. When the fluctuations between p53h and p53w were compared, several differences were observed. First, among the three loops, L1 and L3 were significantly more stable in p53w than in p53h while the stability of loop L2 was comparable between the two structures. Note that the structural difference between the human and worm p53 is that in the worm the three loops consistently contain more helical secondary structure and thus are more stable by themselves and have more contact with the β-sheet frame. This result confirms that the increased secondary structure and additional contacts indeed can lower the fluctuations of the local structure and may also affect the overall stability. On the other hand, the stabilities of loop L2 were similar to each other for the two proteins. One of the reasons for this similarity is that both loops L2 in human and worm contain some helical structure, while the presence of such secondary structural component in loops L1 and L3 was observed only in the worm form. In addition, the conformations of loop L2 were similar for the two proteins while loops L1 and L3 assumed different conformations for the two proteins in their respective crystal structures (*28*). This difference may also have contributed to the difference in fluctuations of the loops.

Table 1: Motif RMSD Comparison between the Human and Worm p53 Averaged over a 5 ns Trajectory[a]

	300 K		325 K	
motif	p53h	p53w	p53h	p53w
S1	**2.1 ± 0.8**	**0.8 ± 0.2**	**1.9 ± 0.5**	**0.8 ± 0.2**
L1	**3.4 ± 2.2**	**1.5 ± 0.4**	**4.2 ± 1.4**	**1.4 ± 0.3**
S2	**1.1 ± 0.6**	**0.7 ± 0.2**	**1.2 ± 0.3**	**0.7 ± 0.2**
S2′	0.9 ± 0.3	0.6 ± 0.2	**1.2 ± 0.3**	**0.6 ± 0.2**
S3	0.9 ± 0.4	0.7 ± 0.2	**1.3 ± 0.2**	**0.6 ± 0.2**
S4	0.7 ± 0.1	0.5 ± 0.1	0.8 ± 0.2	0.6 ± 0.1
L2	**1.8 ± 0.4**	**1.4 ± 0.2**	1.6 ± 0.4	1.5 ± 0.3
H1	**1.9 ± 0.5**	**1.4 ± 0.3**	**2.7 ± 0.5**	**1.6 ± 0.3**
S5	0.8 ± 0.2	0.7 ± 0.2	0.9 ± 0.2	0.7 ± 0.2
S6	1.1 ± 0.3	1.2 ± 0.2	1.3 ± 0.3	1.5 ± 0.5
S7	0.8 ± 0.2	0.8 ± 0.2	0.8 ± 0.2	0.8 ± 0.2
S8	0.7 ± 0.2	0.6 ± 0.1	0.9 ± 0.2	0.7 ± 0.1
L3	1.9 ± 0.4	1.6 ± 0.3	2.4 ± 0.3	2.0 ± 0.4
S9	0.8 ± 0.2	0.6 ± 0.1	0.9 ± 0.2	0.6 ± 0.1
S10	0.9 ± 0.3	0.7 ± 0.1	**1.1 ± 0.2**	**0.6 ± 0.1**
H2	1.8 ± 0.4	1.8 ± 0.5	**2.2 ± 0.4**	**1.4 ± 0.5**
S2S2′	1.0 ± 0.6	1.5 ± 0.6	1.6 ± 0.6	1.6 ± 1.3
S2′S3	**1.3 ± 0.7**	**0.8 ± 0.2**	**1.3 ± 0.4**	**0.8 ± 0.2**
S3S4	1.3 ± 0.4	1.7 ± 0.3	1.1 ± 0.3	1.4 ± 0.3
H1S5	**3.5 ± 1.0**	**1.0 ± 0.2**	**2.8 ± 0.7**	**1.0 ± 0.2**
S5S6	1.2 ± 0.4	0.9 ± 0.2	1.5 ± 0.5	2.3 ± 1.3
S6S7	2.2 ± 0.5	2.0 ± 0.4	1.4 ± 0.6	1.8 ± 0.4
S7S8	**3.5 ± 0.8**	**1.8 ± 0.4**	**4.0 ± 1.2**	**1.3 ± 0.4**
S9S10	**2.0 ± 0.5**	**1.3 ± 0.3**	1.4 ± 0.5	1.2 ± 0.3

[a] The whole trajectory, instead of the last few nanoseconds of the trajectory, was used for the average calculation to reflect the structural deviation from the starting conformations. The RMSD numbers were highlighted in bold if the difference between human and worm p53 was larger than 0.4 Å.

Interestingly, Figure 3 also reveals significant differences in fluctuations for other structural motifs between the two proteins, such as the turns that link the β-strands or β-strands and helix. Notably, the segments between S7 and S8 (referred to as turn S7S8) and between H1 and S5 (turn H1S5) were much more unstable in p53h than in p53w. Comparison of the structures shows that, in addition to the differences in the loops, both turns S7S8 and H1S5 in p53w are much shorter than in the human p53. These two turns, particularly turn S7S8, were not well packed against the β-sheet scaffold in the human p53 and therefore were very mobile. The locations of these two turns were highlighted in Figure 1.

To further characterize whether these flexible motifs actually result in the instability, the average RMSD for the motifs were calculated at 300 and 325 K, respectively. The RMSD for each secondary structural motif, including the loops and turns, gives a more quantitative description of the contribution of the structural component to the stability of the core domain. The data in Table 1 show that, at 300 K, structural motifs that were significantly less stable in p53h than in p53w include strand S1, loop L1, and turns H1S5, S7S8, and S9S10 (the turn that links strands S9 and S10). These unstable motifs were further confirmed by the simulations at 325 K (Table 1). In addition, by comparing the difference at two temperatures, it is noticeable that regions nearby the most mobile motifs became more mobile, especially in the loop L1 region, as manifested when the simulation temperature was raised from 300 to 325 K. This seems to be the result of propagation of the fluctuation because of their neighboring locations. Therefore, it is reasonable to argue that the fluctuation of these most mobile regions is responsible for the initial unraveling of the proteins that leads to conformational changes or even unfolding upon propagation of the movement.

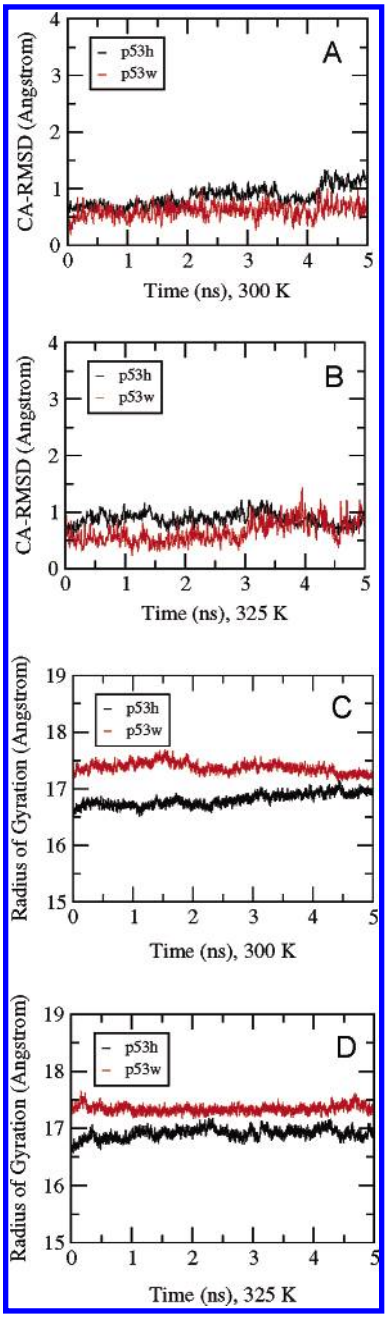

FIGURE 4: Comparison of the β-sheet scaffold stability and the change of the overall molecular shape. (A, B) Cα atom root-mean-square deviations (RMSD) for the β-sheet core part derived from simulations at 300 and 325 K from both the human p53 core domain (p53h) and the worm p53 core domain (p53w) from their crystal structures, respectively. The plots show that the β-sheet core was quite stable for both the human and worm forms, suggesting that conformational changes of the p53 core domain are dominated by the movement of peripheral motifs. (C, D) Changes of the radius of gyration over the 5 ns simulations for both p53h and p53w at 300 and 325 K, respectively. After the initial expansion upon heating, p53h expanded to some extent, while the p53w core domain remained level or even decreased, slightly.

On the other hand, the β-sheet scaffold did not show much fluctuation, and the difference in the fluctuations between the β-sheet scaffolds of p53h and p53w was minimal (Figure 4A,B). At 300 K, the two β-strand scaffolds were stable, and their stabilities are very similar to each other for up to

Table 2: Average Backbone Dihedral Angles for Residues near the Mutation Site for both the Wild Type and the Mutant with Turn S7S8 Deletion[a]

	ϕ dihedral				ψ dihedral			
	300 K		325 K		300 K		325 K	
residue	p53h	mutant	p53h	mutant	p53h	mutant	p53h	mutant
219	−74.3 ± 8.1	−70.5 ± 7.8	−71.5 ± 8.4	−73.4 ± 8.5	158.7 ± 10.2	150.2 ± 11.4	150.1 ± 16.6	159.0 ± 11.6
220	−93.9 ± 15.6	−82.5 ± 10.5	−88.6 ± 14.4	−83.9 ± 12.9	118.4 ± 16.5	126.2 ± 13.9	122.5 ± 18.8	120.4 ± 15.6
221	−110.3 ± 19.0	−114.4 ± 17.9	−116.3 ± 19.8	−103.3 ± 20.0	135.1 ± 20.6	158.5 ± 12.9	120.8 ± 19.4	156.1 ± 13.4
222	−72.4 ± 8.2	−67.1 ± 7.4	−71.9 ± 8.5	−68.9 ± 8.6	158.5 ± 12.2	162.2 ± 12.1	152.6 ± 16.0	168.0 ± 10.8
223	**−75.5 ± 8.3**	**−75.2 ± 12.1**	**−74.8 ± 9.3**	**−73.9 ± 12.7**	**167.8 ± 17.1**	**146.1 ± 10.5**	**168.5 ± 17.8**	**143.9 ± 9.9**
229	**−113.3 ± 24.2**	**−91.4 ± 12.8**	**−101.4 ± 22.9**	**−85.4 ± 14.7**	**176.4 ± 19.0**	**126.0 ± 18.1**	**164.8 ± 20.3**	**125.3 ± 13.8**
230	−102.0 ± 16.1	−109.6 ± 19.2	−117.3 ± 20.3	−105.6 ± 18.1	118.4 ± 12.8	123.7 ± 13.0	128.2 ± 22.7	107.9 ± 19.3
231	−102.5 ± 12.6	−98.4 ± 13.0	−105.7 ± 14.8	−103.0 ± 16.7	120.1 ± 10.8	120.1 ± 11.0	117.8 ± 13.0	119.6 ± 12.0
232	−104.8 ± 10.4	−98.9 ± 10.9	−108.2 ± 12.2	−100.1 ± 12.0	129.8 ± 9.3	126.2 ± 8.4	129.5 ± 8.8	128.2 ± 9.6
233	−99.7 ± 10.8	−97.3 ± 9.6	−96.5 ± 10.2	−98.4 ± 10.2	99.2 ± 11.8	98.8 ± 13.7	101.4 ± 13.5	98.8 ± 13.1

[a] Residues Pro223 and Cys229 were separated by five flexible residues in the human wild-type p53 and were resealed in the mutant. The backbone dihedral angles of these two residues were highlighted in bold.

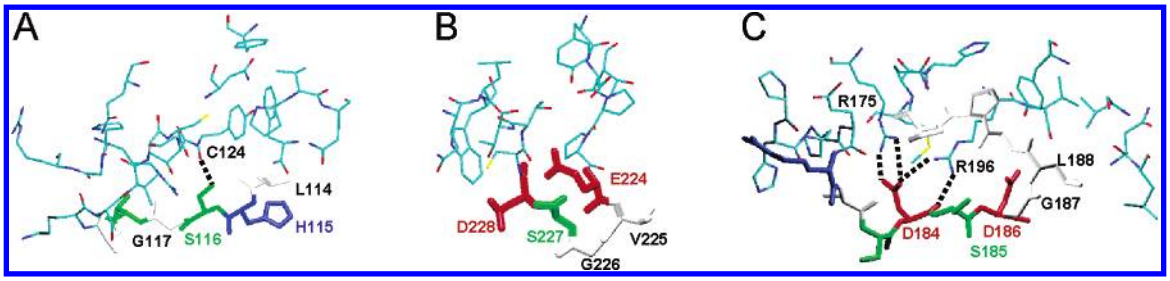

FIGURE 5: Atomic details within 5 Å of the structural motifs of interest: (A) loop L1, (B) turn S7S8, and (C) turn H1S5. The residues in the three motifs were represented with thick lines and colored on the basis of residue types while the surrounding residues were represented with thin lines. Important hydrogen-bonding interactions between the motifs and their surrounding residues were represented with dotted lines. The common feature for the mobile motifs is that they have very limited interactions with their surroundings.

2 ns (Figure 4A). After 2 ns, p53h displayed some instability relative to p53w, possibly due to the movement of the peripheral motifs. Similarly, at 325 K, the two β-sheet cores were still stable, and the difference between their stabilities was small, although some noticeable difference appeared early in the trajectories (Figure 4B). Since the overall difference in structural fluctuations between p53h and p53w was quite dramatic (Figure 2), such a difference between the β-sheet frames was likely to be caused by the early movement of the peripheral motifs in p53h. This difference early in the trajectory, however, disappeared after 3 ns, when p53w also started to unravel, resulting in fluctuations to a similar extent as p53h. This result shows that the β-sheet core was quite stable for both proteins.

Interestingly, the radius of gyration of p53h became larger as the trajectory progressed, as one would have expected for many proteins (Figure 4C,D). However, the radius of gyration for p53w stayed leveled or even became smaller, at both 300 and 325 K (Figure 4C,D). Such a difference in this structural property suggests that peripheral motifs such as turns and loops are very important in the early events of p53 unfolding or for the population of other conformational states, which is responsible for its loss of activity.

Identification of Potential Sites for Stabilizing Mutations. From the result discussed earlier, based on the motif stability difference between the two proteins, several regions are potential targets for mutations, including β-strand S1, loop L1, and turns H1S5, S7S8, and S9S10. Others include β-strands S2, S2′, and S3, loop L2, helices H1 and H2, and turn S2′S3 (Figure 3 and Tables 1 and 2). Among these motifs, only β-strand S1, loop L1, and turns H1S5, S7S8, and S9S10 are less conserved (*26*), and their mutations are noncancerous, based on the mutation database (*5*−*7*). Because strand S1 is near the N-terminus, the fluctuation difference between the two proteins could be caused by the terminal effect and therefore is less interesting for this study. Also, the fluctuations of turn S9S10 and their difference between the two proteins at 325 K were both reduced. Therefore, the most promising regions for stabilization of the human p53 are loop L1 and turns H1S5 and S7S8. These structural motifs were highlighted in red or cyan in Figure 1.

The common feature for the above three motifs is that they either pack loosely against the core frame with mostly only side chain contacts (loop L1 and turn H1S5) or lack contacts (turn S7S8) (Figure 5). For example, the most flexible region of loop L1 covers residues Leu114, His115, Ser116, and Gly117 (Figure 5A). Among these residues, Leu114 made some loose contact with the Pro242 side chain; the Ser116 side chain made a hydrogen bond with Cys124, and Gly117 formed a hydrogen bond with Thr125. There is no other significant interaction between the loop and the core. In the case of turn S7S8, the most flexible five residues, Glu224, Val225, Gly226, Ser227, and Asp228, stretch out away from the core β-sheet frame and are not in any noticeable contact with the core frame in the crystal structure (see Figures 1 and 5B). The most flexible region in turn H1S5 includes residues Asp184, Ser185, Asp186, Gly187, and Leu188 (Figure 5C). Among the three most mobile motifs, turn H1S5 has the most contact with the protein core. However, most of the contacts were made between the side chains. In addition, this turn sits on top of two charged

residues, Arg175 and Arg196, that reside at the N-terminus of helix α1 and inside β-strand S5, respectively. The side chain of Asp184 from the turn formed a salt bridge with Arg175 while its backbone formed a hydrogen bond with Arg196 (Figure 5C). These hydrogen bonds are potentially venerable since they are at least partially accessible to solvent. From the simulations, it is revealed that part of this turn flipped up, breaking the hydrogen bond between the main chain hydrogen bond acceptor of Asp184, although the salt bridge survived (data not shown).

To design stable functional mutants, detailed analysis of the conformational features is necessary for identifying the potential site for engineering. In our previous work, we have shown that loop L1 can be stabilized by substituting Ser116 with Met, without disturbing the wild-type conformation. In light of the conformation of this loop in the worm p53, one can also engineer the loop to enhance the secondary structure component. In principle, the same approach can be applied to turns S7S8 and H1S5. Because the structural difference between p53h and p53w is that both of these motifs are obviously longer in p53h than in p53w, one can also try to reduce the length of the turns to achieve the stability, especially for turn S7S8. This turn (S7S8) stretches out away from the core β-sheet frame, and the central five residues of the turn are not in any noticeable contact with the core frame in the crystal structure (Figures 1 and 5B). Thus, it will be difficult to introduce a different residue in the turn to increase the packing without changing the turn conformation.

Shortening Turn S7S8 Results in a Stable Mutant p53. Stabilizing the peripheral structural motifs may greatly enhance the overall stability of a protein. We have shown previously that the core domain conformation is well retained when loop L1 is stabilized by substituting Met for Ser116. To test whether this hypothesis holds, we tried to stabilize a different motif, turn S7S8, to see its impact on the overall stability of p53 by simply reducing the size of the turn. This turn resides in the vicinity of loop L1 (Figure 1) and is located on the opposite side of the DNA binding interface. In the DNA−p53 complex model that assumes that four copies of p53 core domains specifically bind to the 20 base pair DNA full site with the consensus sequence, this turn is not involved in the dimerization interface. The role of turn S7S8 in the context of the tetramer is not clear, although it may have some role in the dimer−dimer interface of the core domains. However, such interactions might not be significant because the p53 specific binding to the consensus full site of the DNA with base pair insertions can be as strong and cooperative as its binding to such a DNA site without insertions.

Structure-based sequence alignment shows that there are three more residues (Glu224, Val225, and Gly226) in turn S7S8 of p53h than in the turn of p53w and no residue conservation between the two proteins is revealed for the turn region except for residue Pro222. Therefore, it would be reasonable to delete the three extra residues when comparing the stability difference before and after the deletion. Further analysis of the structure of turn S7S8 and its flexibility shows that the central five residues, Glu224, Val225, Gly226, Ser227, and Asp228, are essentially isolated from the rest of the protein and are assumed to be responsible for the high fluctuation of the turn (Figures 3A and 5B). The only contact for these five residues is among their main chain atoms. The reason that the S7S8 turn in p53h has five extra residues instead of three as suggested by the structure-based sequence alignment is the different distances between strands S7 and S8 in the two proteins. The distance between S7 and S8 (especially the distance between the residues that directly flank turn S7S8) in p53h is shorter than that in p53w (data not shown), which leaves the other two residues, Ser227 and Asp228, in p53h having no counterpart in p53w.

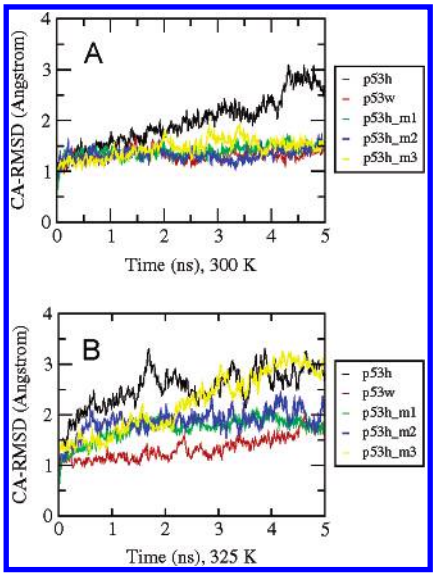

FIGURE 6: Cα atom root-mean-square deviations (RMSD) derived from simulations at 300 and 325 K for wild-type human p53 (p53h), worm p53 (p53w), human form mutants designed in this work (p53h_m1), human p53 mutant with S116M substitution in loop L1 (p53h_m2), and the quadruple mutant (p53h_m3) from the wild-type crystal structures, respectively. The plots show that the worm form p53 (p53w) was the most stable. They also reveal that both the turn S7S8 mutant (p53h_m1) and the loop L1 mutant (p53h_m1) were more stable than the quadruple mutant (p53h_m3). The three terminal residues at both the N- and C-termini were excluded in the calculations.

On the basis of the discussion above, we designed a mutant by shortening turn S7S8. Specifically, we simply cut off the central five residues (Glu224, Val225, Gly226, Ser227, and Asp228). In addition, a P223A mutation was introduced to facilitate the connection between residues Pro223 and Cys229 after the deletion of the five residues. The mutant was built by resealing the mutated residues Ala223 and Cys229, which was then subjected to molecular dynamics simulations to evaluate its stability. Note that Pro223 which we have mutated to Ala is a conserved residue. The position of Pro223 in the wild type suggests that this residue may be present for the purpose of restraining the propagation of the movement from turn S7S8 and therefore to maintain the stability of the core domain. Therefore, we argue that such mutations should not impose a detrimental effect on the function of the protein.

Figure 6 shows the RMS deviations of the mutant along with those of the wild type and several other variants and that of the worm p53. Remarkably, the RMS deviation of the mutant became very small and stable over the 5 ns trajectory at 300 K, which is comparable with the S116M mutant and the quadruple mutant (M133L/V203A/N239Y/N268D) designed previously (*25*, *32*) and is only slightly less stable than p53w (Figure 6A). At 325 K, the mutant was still able to retain its conformation, and the deviation

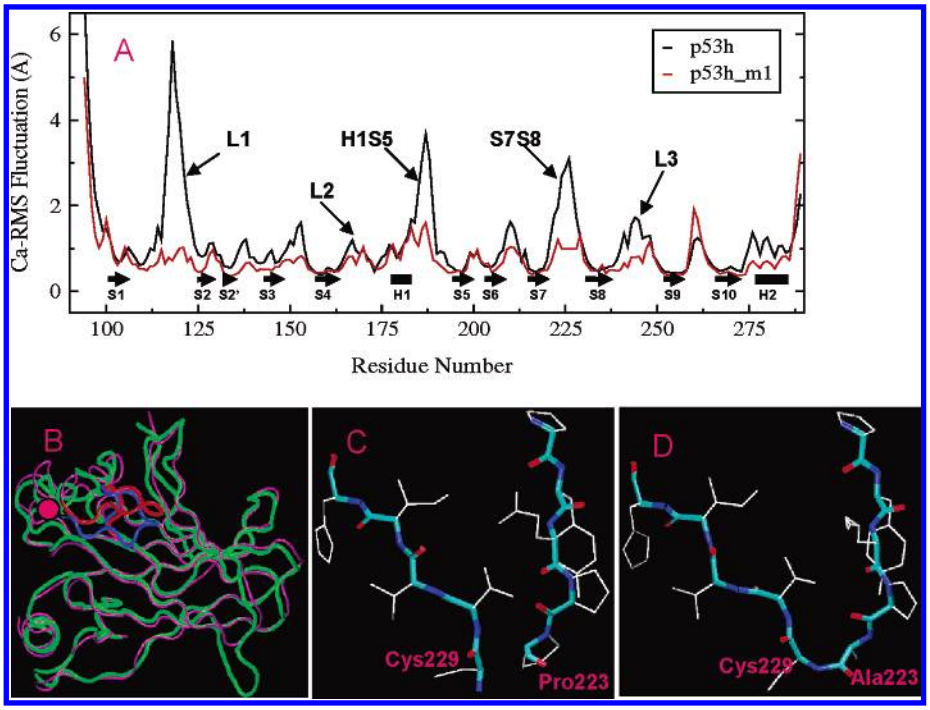

FIGURE 7: Structural properties of the S7S8 turn mutant in comparison with the wild type. (A) Residue-based Cα RMS fluctuations for the wild type and the S7S8 turn mutant of the human p53 derived from the 5 ns simulations. Secondary structures were labeled the same way as in Figure 3. The data here show a great impact of the mutation on the overall stability of the protein, with the flexibility reduced in most mobile regions, including loop L1 and turn H1S5. (B) The backbone trace of the mutant structure averaged over the 5 ns trajectory superimposed on that of the wild-type crystal structure. (C) The atomic detail conformation of the turn S7S8 region in the wild-type crystal structure. The five residues at the center of the turn were not shown. (D) The atomic detail conformation of the turn S7S8 region in the mutant average structure. This result shows that, upon mutation, the stability of the protein was greatly increased and the native conformation was well retained by the mutation.

was only about 1.7 Å from the wild-type crystal structure. This mutant is more stable than the S116M mutant and much more stable than the quadruple mutant based on the simulations (Figure 6B). The reduction in overall fluctuation is also attributable to the low fluctuation in the loop L1 region. Some motional correlation between loop L1 and turn S7S8 was observed previously, and therefore it is possible that the stabilization of loop L1 was partly due to the stabilization of turn S7S8.

Figure 7A shows the residue-based fluctuations of the mutant in comparison with the wild type. It is remarkable to observe that the stabilization was across the entire sequence, most significantly in the loop L1 and the turn H1S5 region. Comparison with the quadruple mutant and our previously designed S116M mutant shows that the reduction in fluctuation is more significant here, while in the S116M mutant, the fluctuations in the H1S5 and S7S8 turn regions were reduced slightly (data not shown). As a result, superposition of the mutant p53 snapshot at the end of the simulation onto the wild-type crystal structure shows little overall conformational change (Figure 7B). Locally, the distance between the Cα atom of residue Pro222 and that of residue Thr120 changed by only 0.1 Å (from 6.2 to 6.1 Å). The two reconnected residues, Ala223 and Cys229, rotated slightly to fit with each other (Figure 7C,D). This result shows that the structural perturbation caused by the deletion mutation is minimal in this case. Overall, these results suggest that the stability of the S7S8 turn has a greater impact on the overall stability of the core domain.

Validation of the Stabilization. To ensure that the stability is not an artifact due to the constraint imposed by the connection between Ala223 and Cys229 in the mutant, the backbone ϕ/ψ conformational space for five residues preceding Ala223 and five residues following Cys229 was measured and compared with that of the wild type. These residues' movement would have been influenced the most by the constraint introduced due to the mutation if any. From Table 2 one can see that the conformational space for each residue remained essentially the same before and after the mutation, except for the two residues directly next to the deleted segment and residue Glu221. The extents of fluctuations of the dihedral angles were also very similar before and after the deletion, except for the three residues mentioned earlier.

The local adjustment of the conformation to adapt to the new environment is noticeable for residues Glu221, Pro222, Pro223Ala, and Cys229. Both residues Ala223 (after the mutation) and Cys229 rotated toward each other. Because the backbone of Pro222 is quite rigid, the consequence of the Ala223 rotation was transferred to Glu221. In addition, the dynamics also allowed better interactions between Glu221 and Lys202 to make a salt bridge. The average shortest distance between the side chains of Glu221 and Lys202 changed from 3.65 to 2.60 Å, which is also partially responsible for the conformational change of Glu221. However, the most significant local conformational change was in residue Cys229. The ϕ and ψ dihedral angles for this residue changed by about 20° and 40°, respectively. From Figure 7C,D, it can be seen that the side chain of this residue is not in contact with other structural motifs, and therefore such a conformational change can happen readily. The fluctuation of the conformational space for this residue is

comparable before and after the mutation. The only noticeable reduction in the conformational space is for the ψ dihedral angle of residue Ala223 (the reduction of the dihedral angle deviation; Table 2). However, the fluctuation of the ϕ dihedral angle was slightly increased, compensating for the reduced freedom of the ψ dihedral space.

DISCUSSION AND CONCLUSIONS

In the past several years many efforts focused on the rescue of the p53 native conformation. A recent study on crystal structures of different mutants has shown that cancerous mutations either disrupt the local conformations at the DNA binding interface or significantly destabilize the native structure (*36*). Because the mutations can be mapped onto the wild-type core domain and their stabilization effects can be rationalized on a chemical basis, it is now clear that if a mutation can enhance the overall stability and still maintain the conformation at the DNA binding surface, such a structural modification is likely to increase the DNA binding affinity. Therefore, based on the same principle, a residue whose mutation is involved in cancer can also be engineered for stabilization. For example, the quadruple mutant M133L/V203A/N239Y/N268D involved mutations of residues Met133 and Asn239, which are cancerous on their own. Yet, this quadruple mutant was proved to be stable and functional. Thus, the impact of such cancerous mutations is mainly on the stability and not their direct involvement in DNA binding.

In this paper, we have compared the stability differences between the human p53 and worm p53 for each corresponding structural motif. Several motifs were characterized as potential targets for stabilization. Because they are not in direct contact with DNA in the crystal complex structure, stable mutants created by modifying these regions are believed to have a good chance to maintain the p53 affinity for DNA binding and its transcriptional function. The mutant designed in this work involved the deletion of five residues and a substitution of another in turn S7S8. Among these deleted/mutated residues, Pro223 and Glu224 mutations were cancerous by themselves. Because the deletion of the five residues is likely to enhance the stability of the protein, as was shown in the simulations, the original single mutational effect could be compensated by the enhancement of the overall stability.

Allosteric effects have been suggested to be a universal mechanism for the conjugation of conformational change of different motifs. For the p53 core domain, the correlation of movement between loop L1 and turn S7S8 was observed previously (*32*). Upon stabilization of loop L1, the fluctuation of turn S7S8 was also reduced. Similarly, after the deletion of part of turn S7S8, the fluctuation of loop L1 dropped dramatically (Figure 7). Because loop L1 is crucial for DNA binding, the effect of a change in the stability of turn S7S8 on the DNA binding can help us to understand the DNA binding mechanism or the conformational requirements. For example, shortening the turn by a different number of residues will potentially lead to different flexibilities that would allow the movement of the loops to different extents. It would be interesting to see whether the very stable mutant with the shortened turn S7S8 still has a similar DNA binding affinity and subsequent transcriptional activities. If our mutant model proves to be thermodynamically stable, the relationship between its stability and the DNA binding affinity can also shed light on the conformational requirement for DNA binding and the flexibility of p53. One interesting phenomenon observed in the simulation is that both our modeled mutants S116M and deletion of turn S7S8 have much lower structural fluctuations than the experimentally proved superstable quadruple mutant. It seems that the single point mutations or their combination in the central region allows more overall flexibility than mutations in the peripheral motifs, which tend to reduce the flexibility of the molecule to a larger extent. If the stabilities observed in our simulations are validated experimentally, then such an approach can also be used to study the correlations between flexibility and function and the role of these peripheral motifs in allosteric effects.

A related question is to what extent the p53 protein should be stabilized in order to function at its optimal level. The simulations, especially those at high temperature, reveal that the worm p53 is more stable than the human p53 and all of the stable human p53 mutants. Since the worm p53 is functional in transcriptional activity, it seems that the further stabilization does not necessarily hamper its function. This suggests that there is still room for improvement in the stability of the human p53 for therapeutic purposes. Therefore, the stability achieved here by deletion of the turn seems to be reasonable. On the other hand, it is also interesting to note that the free form and the DNA-bound form p53 have almost the same conformation. That is, the deformation of p53 upon DNA binding is very limited. However, the high flexibility and low stability of p53 is thought to result from its involvement in many cellular processes. Therefore, while excessively reducing the flexibility of the protein may enhance the DNA binding affinity, it may also adversely affect other roles of the protein. The interplay among the stability, flexibility, and conformational change upon DNA binding can be better understood when our computationally designed mutants are structurally and functionally tested by experiments.

In summary, we have compared the stabilities of the core domains of the human and the worm p53 proteins. On the basis of the behavior of the structural fluctuations, we propose that the peripheral structural motifs, such as loops and turns that are usually loosely packed against the core, are the major factors leading to the initial conformational changes and unfolding. On the basis of this proposition, and borrowing ideas from nature's design for the worm p53, we designed a stable human form mutant by shortening a turn between β-strands S7 and S8. This type of stable mutant not only is important as a potential therapeutic agent but also may be useful in probing the structural and functional role of the flexible motifs. Our results further provide insight into allosteric effects in p53. The higher stability of turn S7S8 stabilizes loop L1 and thus is likely to affect DNA binding affinity.

REFERENCES

1. Bargonetti, J., and Manfredi, J. J. (2002) Multiple roles of the tumor suppressor p53, *Curr. Opin. Oncol. 14*, 86−91.
2. Kastan, M. B., Onyekwere, O., Sidransky, D., Vogelstein, B., and Craig, R. W. (1991) Participation of p53 protein in the cellular response to DNA damage, *Cancer Res. 51*, 6304−6311.
3. Polyak, K., Xia, Y., Zweier, J. L., Kinzler, K. W., and Vogelstein, B. (1997) A model for p53-induced apoptosis, *Nature 389*, 300−305.

4. Chan, T. A., Hermeking, H., Lengauer, C., Kinzler, K. W., and Vogelstein, B. (1999) 14-3-3Sigma is required to prevent mitotic catastrophe after DNA damage, *Nature 401*, 616−620.
5. Beroud, C., and Soussi, T. (1998) p53 gene mutation: software and database, *Nucleic Acids Res. 26*, 200−204.
6. Hainaut, P., and Hollstein, M. (2000) p53 and human cancer: the first ten thousand mutations, *Adv. Cancer Res. 77*, 81−137.
7. Hollstein, M., Rice, K., Greenblatt, M. S., Soussi, T., Fuchs, R., Sorlie, T., Hovig, E., Smith-Sorensen, B., Montesano, R., and Harris, C. C. (1994) Database of p53 gene somatic mutations in human tumors and cell lines, *Nucleic Acids Res. 22*, 3551−3555.
8. Bullock, A. N., Henckel, J., DeDecker, B. S., Johnson, C. M., Nikolova, P. V., Proctor, M. R., Lane, D. P., and Fersht, A. R. (1997) Thermodynamic stability of wild-type and mutant p53 core domain, *Proc. Natl. Acad. Sci. U.S.A. 94*, 14338−14342.
9. Bargonetti, J., Manfredi, J. J., Chen, X., Marshak, D. R., and Prives, C. (1993) A proteolytic fragment from the central region of p53 has marked sequence-specific DNA-binding activity when generated from wild-type but not from oncogenic mutant p53 protein, *Genes Dev. 7*, 2565−2574.
10. Hinds, P. W., Finlay, C. A., Quartin, R. S., Baker, S. J., Fearon, E. R., Vogelstein, B., and Levine, A. J. (1990) Mutant p53 DNA clones from human colon carcinomas cooperate with ras in transforming primary rat cells: a comparison of the "hot spot" mutant phenotypes, *Cell Growth Differ. 1*, 571−580.
11. Stephen, C. W., and Lane, D. P. (1992) Mutant conformation of p53. Precise epitope mapping using a filamentous phage epitope library, *J. Mol. Biol. 225*, 577−583.
12. Gannon, J. V., Greaves, R., Iggo, R., and Lane, D. P. (1990) Activating mutations in p53 produce a common conformational effect. A monoclonal antibody specific for the mutant form, *EMBO J. 9*, 1595−1602.
13. Soussi, T., and May, P. (1996) Structural aspects of the p53 protein in relation to gene evolution: a second look, *J. Mol. Biol. 260*, 623−637.
14. Soussi, T., Caron de Fromentel, C., and May, P. (1990) Structural aspects of the p53 protein in relation to gene evolution, *Oncogene 5*, 945−952.
15. Friedler, A., DeDecker, B. S., Freund, S. M., Blair, C., Rudiger, S., and Fersht, A. R. (2004) Structural distortion of p53 by the mutation R249S and its rescue by a designed peptide: implications for "mutant conformation", *J. Mol. Biol. 336*, 187−196.
16. Soussi, T., Caron de Fromentel, C., Mechali, M., May, P., and Kress, M. (1987) Cloning and characterization of a cDNA from *Xenopus laevis* coding for a protein homologous to human and murine p53, *Oncogene 1*, 71−78.
17. Kato, S., Han, S. Y., Liu, W., Otsuka, K., Shibata, H., Kanamaru, R., and Ishioka, C. (2003) Understanding the function-structure and function-mutation relationships of p53 tumor suppressor protein by high-resolution missense mutation analysis, *Proc. Natl. Acad. Sci. U.S.A. 100*, 8424−8429.
18. Bykov, V. J., Issaeva, N., Shilov, A., Hultcrantz, M., Pugacheva, E., Chumakov, P., Bergman, J., Wiman, K. G., and Selivanova, G. (2002) Restoration of the tumor suppressor function to mutant p53 by a low-molecular-weight compound, *Nat. Med. 8*, 282−288.
19. Friedler, A., Hansson, L. O., Veprintsev, D. B., Freund, S. M., Rippin, T. M., Nikolova, P. V., Proctor, M. R., Rudiger, S., and Fersht, A. R. (2002) A peptide that binds and stabilizes p53 core domain: chaperone strategy for rescue of oncogenic mutants, *Proc. Natl. Acad. Sci. U.S.A. 99*, 937−942.
20. Yang, Y., Ludwig, R. L., Jensen, J. P., Pierre, S. A., Medaglia, M. V., Davydov, I. V., Safiran, Y. J., Oberoi, P., Kenten, J. H., Phillips, A. C., Weissman, A. M., and Vousden, K. H. (2005) Small molecule inhibitors of HDM2 ubiquitin ligase activity stabilize and activate p53 in cells, *Cancer Cell 7*, 547−559.
21. Nikolova, P. V., Wong, K. B., DeDecker, B., Henckel, J., and Fersht, A. R. (2000) Mechanism of rescue of common p53 cancer mutations by second-site suppressor mutations, *EMBO J. 19*, 370−378.
22. Wright, J. D., Noskov, S. Y., and Lim, C. (2002) Factors governing loss and rescue of DNA binding upon single and double mutations in the p53 core domain, *Nucleic Acids Res. 30*, 1563−1574.
23. Matsumura, I., and Ellington, A. D. (1999) In vitro evolution of thermostable p53 variants, *Protein Sci. 8*, 731−740.
24. Nikolova, P. V., Henckel, J., Lane, D. P., and Fersht, A. R. (1998) Semirational design of active tumor suppressor p53 DNA binding domain with enhanced stability, *Proc. Natl. Acad. Sci. U.S.A. 95*, 14675−14680.
25. Joerger, A. C., Allen, M. D., and Fersht, A. R. (2004) Crystal structure of a superstable mutant of human p53 core domain. Insights into the mechanism of rescuing oncogenic mutations, *J. Biol. Chem. 279*, 1291−1296.
26. Cho, Y., Gorina, S., Jeffrey, P. D., and Pavletich, N. P. (1994) Crystal structure of a p53 tumor suppressor-DNA complex: understanding tumorigenic mutations, *Science 265*, 346−355.
27. Shiraishi, K., Kato, S., Han, S. Y., Liu, W., Otsuka, K., Sakayori, M., Ishida, T., Takeda, M., Kanamaru, R., Ohuchi, N., and Ishioka, C. (2004) Isolation of temperature-sensitive p53 mutations from a comprehensive missense mutation library, *J. Biol. Chem. 279*, 348−355.
28. Huyen, Y., Jeffrey, P. D., Derry, W. B., Rothman, J. H., Pavletich, N. P., Stavridi, E. S., and Halazonetis, T. D. (2004) Structural differences in the DNA binding domains of human p53 and its *C. elegans* ortholog Cep-1, *Structure (Cambridge) 12*, 1237−1243.
29. Schumacher, B., Hanazawa, M., Lee, M. H., Nayak, S., Volkmann, K., Hofmann, E. R., Hengartner, M., Schedl, T., and Gartner, A. (2005) Translational repression of *C. elegans* p53 by GLD-1 regulates DNA damage-induced apoptosis, *Cell 120*, 357−368.
30. Schumacher, B., Schertel, C., Wittenburg, N., Tuck, S., Mitani, S., Gartner, A., Conradt, B., and Shaham, S. (2005) *C. elegans* ced-13 can promote apoptosis and is induced in response to DNA damage, *Cell Death Differ. 12*, 153−161.
31. Schumacher, B., Hofmann, K., Boulton, S., and Gartner, A. (2001) The *C. elegans* homolog of the p53 tumor suppressor is required for DNA damage-induced apoptosis, *Curr. Biol. 11*, 1722−1727.
32. Pan, Y., Ma, B., Venkataraghavan, R. B., Levine, A. J., and Nussinov, R. (2005) In the quest for stable rescuing mutants of p53: computational mutagenesis of flexible loop L1, *Biochemistry 44*, 1423−1432.
33. Brooks, B. R., Bruccoleri, R. E., Olafson, B. D., States, D. J., Swaminathan, S., and Karplus, M. (1983) CHARMM: a program for macromolecular energy, minimization, and dynamics calculations, *J. Comput. Chem. 4*, 187−217.
34. MacKerell, A. D., Jr., Bashford, D., Jr., Bellott, M., Dunbrack, R. L., Jr., Evanseck, J. D., Field, M. J., Fischer, S., Gao, J., Guo, H., Ha, S., Joseph-McCarthy, D., Kuchnir, L., Kuczera, K., Lau, F. T. K., Mattos, C., Michnick, S., Ngo, T., Nguyen, D. T., Prodhom, B., Reiher, W. E., III, Roux, B., Schlenkrich, M., Smith, J. C., Stote, R., Straub, J., Watanabe, M., Wiorkiewicz-Kuczera, J., Yin, D., and Karplus, M. (1998) All-atom empirical potential for molecular modeling and dynamics studies of proteins, *J. Phys. Chem. B 102*, 3586−3616.
35. Jorgensen, W. L., Chandrasekhar, J., Madura, J. D., Impey, R. W., and Klein, M. L. (1983) Comparison of simple potential functions for simulating liquid water, *J. Chem. Phys. 79*, 926−935.
36. Joerger, A. C., Ang, H. C., Veprintsev, D. B., Blair, C. M., and Fersht, A. R. (2005) Structures of p53 cancer mutants and mechanism of rescue by second-site suppressor mutations, *J. Biol. Chem. 280*, 16030−16037.

BI052242N